Indoor Radio Channel Characterization and Modeling for a 5.2-GHz Bodyworn Receiver

K. I. Ziri-Castro, W. G. Scanlon, *Member, IEEE*, and N. E. Evans

***Abstract*—Wireless local area network applications may include the use of bodyworn or handportable terminals. For the first time, this paper compares measurements and simulations of a narrowband 5.2-GHz radio channel incorporating a fixed transmitter and a mobile bodyworn receiver. Two indoor environments were considered, an 18-m long corridor and a 42-m^2 office. The modeling technique was a site-specific ray-tracing simulator incorporating the radiation pattern of the bodyworn receiver. In the corridor, the measured body-shadowing effect was 5.4 dB, while it was 15.7 dB in the office. First- and second-order small-scale fading statistics for the measured and simulated results are presented and compared with theoretical Rayleigh and lognormal distributions. The root mean square error in the cumulative distributions for the simulated results was less than 0.74% for line-of-sight conditions and less than 1.4% for nonline-of-sight conditions.**

***Index Terms*—Bodyworn antennas, channel characterization, finite-difference time-domain (FDTD), radio propagation, ray tracing.**

I. Introduction

WIRELESS local area networking systems, such as HiperLAN type 2 and IEEE 802.11a, operate at 5 GHz and provide high bandwidth services within the indoor environment. Although most terminal equipment will be designed for stationary use, future applications will include bodyworn or handportable devices. Under these close proximity conditions the terminal's radiation pattern is significantly distorted by coupling to the user's body and additional signal attenuation may occur. These effects are not only frequency dependent but will vary with the design of the terminal, its antenna and the exact positioning with respect to the body surface [1]. Under the multipath conditions present in the indoor environment, the distorted radiation pattern of the bodyworn terminal can be considered as a form of spatial filter.

Several multipath models have been suggested to explain the observed statistical nature of the mobile channel. Many researchers have also evaluated electromagnetic interactions between the human body and handset antennas or portable devices [2], [3]. In [3], Toftgard *et al.* show the effect of the human body on the performance of antennas for hand-held portable telephones. They suggest that an average system loss of 3–4 dB should be considered in the link budget and point out that there is considerable fading when users move around in a natural manner. This work compares measurements and ray-tracing simulations in a narrowband indoor propagation channel at 5.2 GHz for a bodyworn terminal moving at a moderate walking speed of 0.5 m/s. Practical signal-level results were obtained using a bodyworn power-measurement receiver and datalogger.

Manuscript received December 10, 2003; revised June 10, 2004.

K. I. Ziri-Castro and W. G. Scanlon are with the School of Electrical and Electronic Engineering, The Queen's University of Belfast, Belfast BT9 5AH, Northern Ireland (e-mail: w.scanlon@ee.qub.ac.uk).

N. E. Evans is with the School of Electrical and Mechanical Engineering, University of Ulster, Newtownabbey BT37 0QB, Northern Ireland.

Digital Object Identifier 10.1109/LAWP.2004.836119

TABLE I
SPECIFICATION AND MEASURED RF PERFORMANCE OF CUSTOM RECEIVER

Parameter	Value	Comment
IF	915 MHz	Single conversion (25 MHz bandwidth)
Front end gain	20.2 dB	Includes loss for bandpass filters and mixer
Calculated NF	4 dB	Effective noise floor of –96 dBm
IF Detector type	Logarithmic	Analog Devices AD8313
Range of P_{in} for linear output	–23 dBm to –88 dBm	65 dB dynamic range (+/− 1 dB error)
Output sensitivity	46 mV/dB	V_{out}: 1.2 V to 4.6 V
Output jitter	+/- 2 mV	Equivalent to 0.04 dB

II. Measurement System

The transmitter (TX) consisted of an R&S SMIQ03B signal generator, a GaAs frequency doubler (Hittite HMC189MS8), a GaAs InGaP power amplifier (Hittite HMC406MS8G), and a sleeve dipole antenna (+2.2 dBi, Mobile Mark model PSTN3-5250). The transmitter was adjusted to deliver +15 dBm to the antenna's input port, taking account of cable losses. The radiating system was placed on a wheeled cart to facilitate movement around the selected measurement locations. The transmit antenna was vertically polarized and mounted 1.35 m above floor level on a wooden support. The bodyworn module (RX) consisted of a custom 5.2-GHz measurement receiver (RX), a 12-bit analog-to-digital converter (ADC) and a notebook PC for data recording. The receive antenna was a sleeve dipole identical to that used at the TX. The RX unit was built as a portable device enclosed in a $150 \times 80 \times 50$ mm conducting box; it delivered an output voltage linear with input power measured in dBm. The specification and measured RF performance parameters are given in Table I. The received power indication from the receiver was sampled at 10-ms intervals using the 12-bit ADC and the results stored on the notebook PC.

Two indoor scenarios were considered, both situated on the fifth floor of a university building. Location 1 was a 1.3 m $\times$ 18 m corridor, and location 2 was a 6 $\times$7-m rectangular office (Fig. 1). The measurement environments were relatively complex, i.e., metallic ducting and lockers set into the corridor walls and fluorescent lighting in the office. For convenience, however, the ray-tracing simulations assumed a regular geometric structure with the following material parameters: walls, relative permittivity 4.0, conductivity 0.001 S/m; for the floor and ceilings, relative permittivity 2.7 and conductivity 0.005 S/m.

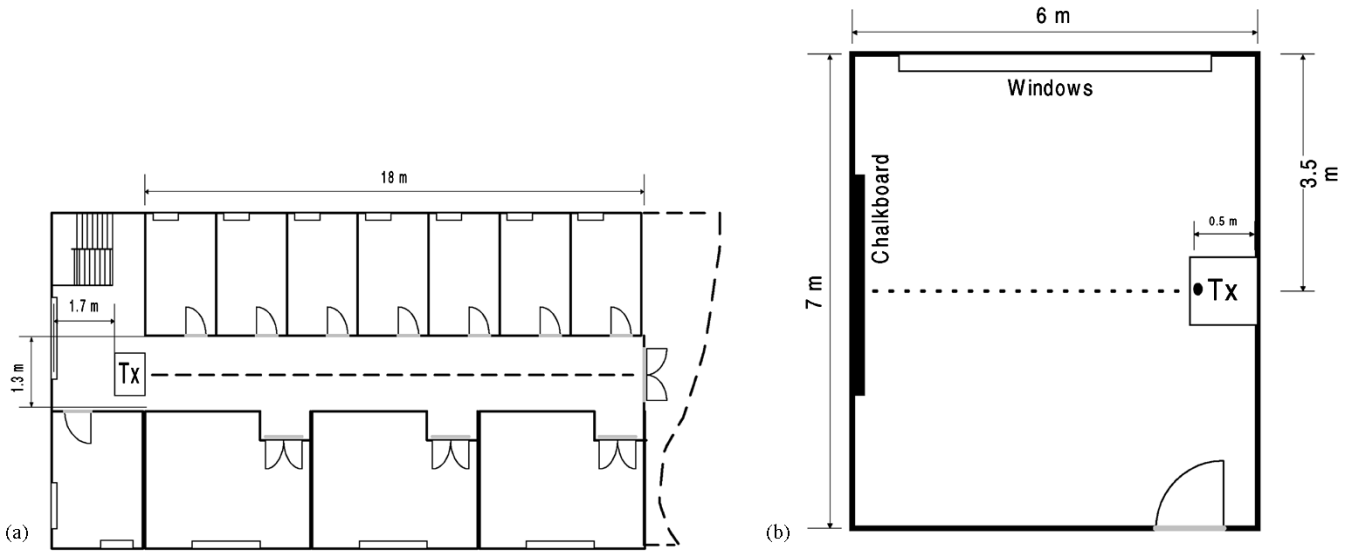

Fig. 1. Measurement locations. (a) Location 1 (corridor). (b) Location 2 (small room). Trajectories are shown dotted.

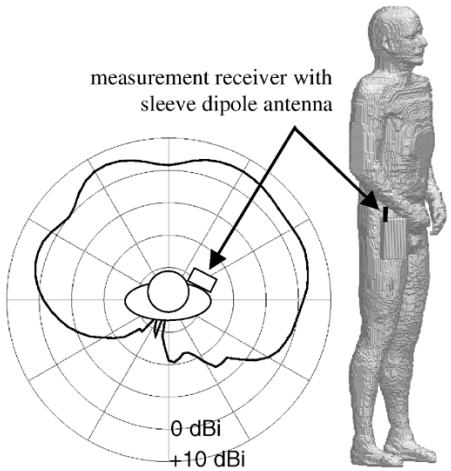

Fig. 2. Finite-difference time-domain (FDTD) computational model and calculated azimuthal radiation pattern (E_θ).

Measurements were performed by fixing the transmitter as shown in Fig. 1 and recording received power using the measurement receiver described above. The RX unit was positioned toward the front of the user's body at the hip (see Fig. 2), while the ADC circuitry and notebook PC were carried in a backpack. Two types of measurement were recorded in both locations: LOS, where the user was walking toward the transmitter, and NLOS, with the user walking away. In all scenarios the user walked along the trajectories shown in Fig. 1, at approximately 0.5 m/s. Therefore, the selected sampling interval of 10 ms corresponds to a spatial resolution of better than $\lambda/11$.

III. Simulation Model

A three-dimensional (3-D) image-based propagation prediction technique [4] was used; although this is capable of modeling the effect of pedestrian movement within the indoor environment, pedestrians were excluded from the present study. Human body proximity effects were included in the simulation as the receiver's polar pattern was obtained from FDTD modeling of the complete bodyworn system. The FDTD model was composed of a human body phantom, conducting box (representing the receiver) and a thin-wire dipole antenna (Fig. 2). The overall FDTD grid was $499 \times 93 \times 154$ with cubic 3.6-mm voxels. The body phantom was for a 1.75-m tall adult male and incorporated 21 tissue types. The sleeve-dipole antenna was modeled as a centre-fed 25.2-mm (0.36-mm radius) thin-wire element with a minimum antenna-body spacing of 14.4 mm. Body losses were relatively low, with an FDTD-computed radiation efficiency of 83.3% at 5.2 GHz. Fig. 2 also shows the calculated azimuthal pattern for vertical polarization (E_θ). The entire 3-D radiation pattern was generated for 5° intervals of both azimuth and vertical angles.

IV. Results

A. General Observations

An example of the measured and received power profiles is given in Fig. 3 for both LOS and NLOS conditions in location 1. The correlation between measurements and simulations for these results was better in the LOS case, with a correlation coefficient of 0.52, than for NLOS, where the corresponding value was 0.25. Table II compares the overall body-shadowing effect (the difference between mean LOS and NLOS powers) obtained through measurement and simulation for both locations. Body-shadowing is dominated by attenuation of the direct ray, caused by reduced antenna gain in the through-body direction. However, it is worthwhile noting that the measured body-shadowing effect (15.7 dB) was significantly more severe in location 2 than in location 1. The variation in body shadowing effect between locations suggests that the propagation channel is strongly influenced by the characteristics of the immediate environment.

There is a low correlation between the overall NLOS measured and simulated received power in both locations, although their mean values are similar. A potential cause of the discrepancy between measurements and simulations is the significant natural variability in the volunteer's posture as he walked. This

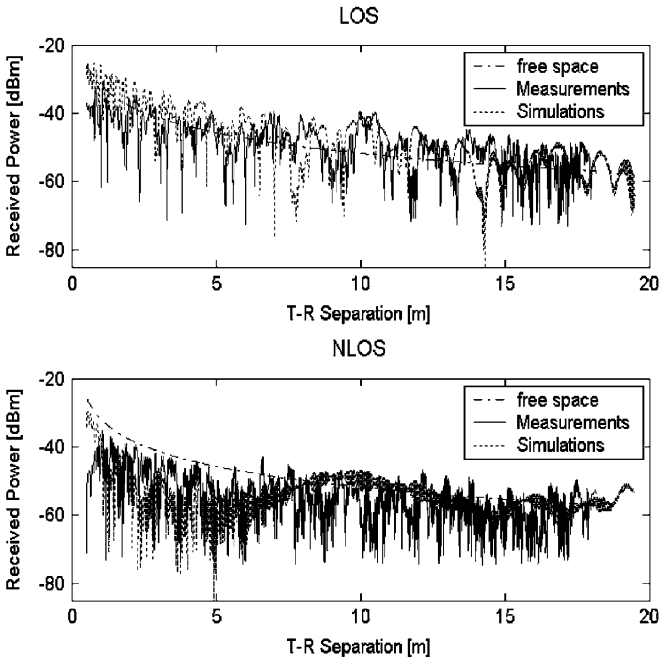

Fig. 3. Measured and simulated received power for location 1 under LOS and NLOS conditions.

TABLE II
COMPARISON OF SIMULATED AND MEASURED RECEIVED POWER AND BODY-SHADOWING EFFECT

Scenario		Measurement	Simulation	Correlation Coefficient Measurement-Simulation
Location 1	LOS Mean (dBm)	–44.6	–39.7	0.52
	NLOS Mean (dBm)	–50.0	–49.5	0.25
	Body-shadowing (dB)	5.4	9.8	-
Location 2	LOS Mean (dBm)	–34.7	–39.4	0.54
	NLOS Mean (dBm)	–50.4	–45.5	–0.05
	Body-shadowing (dB)	15.7	6.1	-

causes a quasi-random variation in the direct ray azimuth angle, leading to rapid fluctuations in ray attenuation. In contrast, the direct ray azimuth angle in the simulation model was constant throughout, with the vertical angle gradually increasing toward the end of the location. The effects of these natural variations in body posture become more significant in NLOS scenarios.

B. First-Order Statistics

All of the statistical measures in this letter correspond to small-scale fading, and were calculated with reference to local mean values (determined by averaging received signal power over 460 samples, $\approx 40\lambda$). The CDF was calculated for the simulated and measured data sets in both locations (Fig. 4). The results were compared to theoretical Rayleigh and lognormal distributions, since it is generally accepted that the received envelope is Rayleigh distributed over a spatial distance of less than 100λ and lognormally distributed over larger areas.

In location 1, LOS measured and simulated CDFs were in good agreement [root-mean square (rms) error of 0.65%] and both were lognormally distributed above the median, while below it they were Rayleigh distributed. However, measured and simulated NLOS results were in less agreement with an rms error of 1.4%. The simulated NLOS results were closer to Rayleigh because of the constant direct ray attenuation

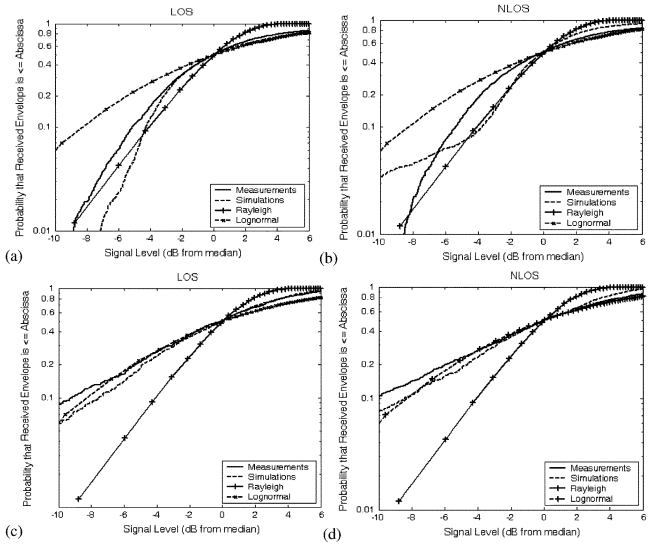

Fig. 4. Small-scale fading cumulative distribution functions (CDFs). (a) Location 1 LOS. (b) Location 1 NLOS. (c) Location 2 LOS. (d) Location 2 NLOS.

described earlier. There was good agreement between measurement and simulation in location 2, with an rms error of 0.74% for the LOS case and 0.87% for the NLOS case, respectively. All measured and simulated CDFs in location 2 were lognormally distributed. Simulation and measurement results from both locations tend to be distributed following a mixture of Rayleigh and lognormal distributions. Some researchers [5], [6] have compared cumulative distributions of experimental data and have suggested the Suzuki distribution, a mixture of the Rayleigh and lognormal distributions, to represent the statistics of mobile radio signals. However, a practical limitation to this distribution is that no closed form has been found to solve the CDF integral [7].

C. Second-Order Statistics

Level-crossing rate (LCR) and average fade duration (AFD) were calculated for both simulated and measured data sets in location 1. Results were compared to theoretical Rayleigh and lognormal distributions with a maximum Doppler frequency, f_m, of 8.67 Hz, which corresponds to a receiver speed of 0.5 m/s.

Although measured and simulated LCR results had similar profiles (Fig. 5), for LOS conditions the peak of the measured LCR curve was 53% higher than that of the simulated curve. Both measured and simulated peak LCR values were significantly higher under NLOS conditions and were comparable to the theoretical Rayleigh maximum LCR. In particular, the simulated results were relatively well matched to the Rayleigh curve. Overall the LCR curves were more similar to Rayleigh than they were to lognormal. Inspection of the raw fading profiles confirmed that the measured results experienced significantly more fading than was predicted by the simulation tool. This suggests that the additional body movements associated with walking led to more rapid envelope variation. As only lateral movement is considered, the simulation tool was unable to faithfully represent these variations. The AFD results [Fig. 5(c) and

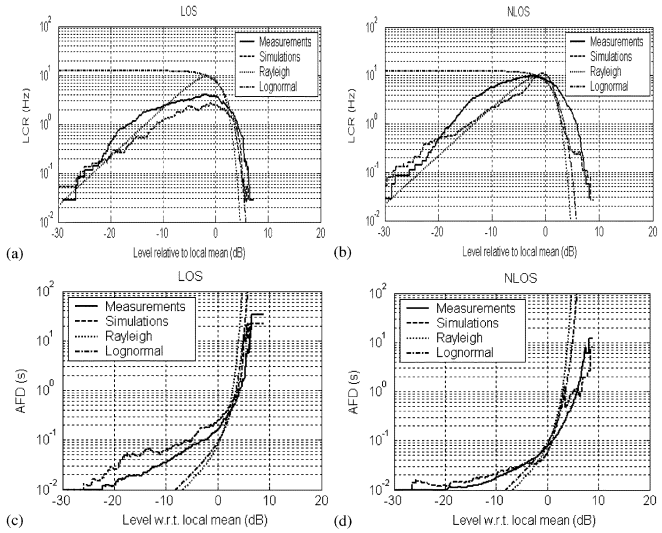

Fig. 5. Second-order statistics for location 1. (a) LOS level crossing rate. (b) NLOS level crossing rate. (c) LOS average fade duration. (d) NLOS average fade duration.

(d)] indicate that the predicted LOS fade duration was consistently longer than that measured. Again, variations in posture or walking speed during measurements may have contributed to these differences.

V. Conclusion

Measurement and simulation results for an indoor narrowband channel using a bodyworn receiver at 5.2 GHz have been presented: body shadowing caused 5–16 dB extra path loss across the locations considered. For small-scale fading, the first-order channel statistics in the corridor tended to be Rayleigh distributed below the mean and lognormally distributed above it, while in the small room, first-order statistics were all lognormally distributed. The second-order statistics in the corridor tended toward Rayleigh even for LOS conditions. The accuracy of the simulation tool used in this work was sufficient in LOS scenarios with an rms error of 0.7% or less in the cumulative distributions. However, it was not suitable for NLOS comparisons due to the inability of the tool to model natural variations in posture during walking. Overall, these results provide an insight into the characteristics of body shadowing for bodyworn terminals in wireless communication systems design at 5 GHz.

References

[1] W. G. Scanlon and N. E. Evans, "Numerical analysis of bodyworn UHF antenna systems," *IEE Electron. Comm. Eng. J.*, vol. 13, pp. 53–64, 2001.

[2] F. L. Lin and H.-R. Chuang, "Performance evaluation of a portable radio close to the operator's body in urban mobile environments," *IEEE Trans. Veh. Technol.*, vol. 49, pp. 614–621, Feb. 2000.

[3] J. Toftgard, S. N. Hornsleth, and J. B. Andersen, "Effects on portable antennas of the presence of a person," *IEEE Trans. Antennas Propagat.*, vol. 41, pp. 739–746, June 1993.

[4] F. Villanese, W. G. Scanlon, N. E. Evans, and E. Gambi, "A hybrid image/ray-shooting UHF radio propagation predictor for populated indoor environments," *Electron. Lett.*, vol. 35, no. 21, pp. 1804–1805, 1999.

[5] H. Suzuki, "A statistical model for urban radio propagation," *IEEE Trans. Commun.*, vol. COMM-25, pp. 673–80, July 1977.

[6] F. Hansen and F. I. Meno, "Mobile radio fading—Rayleigh and lognormal superimposed," *IEEE Trans. Veh. Technol.*, vol. VT-26, pp. 332–335, Apr. 1977.

[7] R. Vaughan and J. B. Andersen, *Channels Propagation and Antennas for Mobile Communications*, London, U.K.: Inst. Elect. Eng., 2003.